RSC Advances

ROYAL SOCIETY OF CHEMISTRY

www.rsc.org/advances

Micropatterning of Nanoenergetic Films of Bi_2O_3/Al for Pyrotechnics

Vinay Kumar Patel, Anurup Ganguli, Rishi Kant and Shantanu Bhattacharya*

Microsystems Fabrication Laboratory, Department of Mechanical Engineering

Indian Institute of Technology Kanpur, Kanpur 208016, Uttar Pradesh, India

*Corresponding author: bhattacs@iitk.ac.in

Tel- +915122596056; fax- +915122597408

Initiatives have been led by researchers all around the world to deposit and pattern nanoenergetic films (nEFs) using various techniques so that printed energetic circuits can be developed for initiation of detonation. In the first module of similar initiative, Bi_2O_3 nano-square-tablets (NSTs) with edge length of ca. 200-300 nm and thickness of *ca.* 50-100 nm were synthesized on gold-sputtered silicon substrate by chemical bath deposition process. Gold nanofilm on Si-substrate was found to act as a catalytic agent for stable colloidal growth of Bi_2O_3 NSTs. In the absence of gold catalyst, micro-leaf structures of Bi_2O_3 were observed to formulate using the same process. The developed Bi_2O_3 NSTs were sputter-coated with aluminum to realize nEFs on Si-substrate. The exothermic reactivity of Bi_2O_3/Al nEFs was evaluated at varied aluminum-sputtering of 60, 100 and 140 nm by TG-DSC measurements from 50 to 800 ^{o}C at heating rate of 10 ^{o}C /min under nitrogen environment. The nEFs formulated with 140 nm aluminum-sputtering has developed highest heat of reaction of 710 J/g at initiation temperature of 535 ^{o}C in TG-DSC measurement and when burnt in a constant-volume pressure-cell, developed peak pressure of 40.8 MPa and pressurization rate of 4.08 MPa μs^{-1}. In the final module, we have been able to pattern the Bi_2O_3/Al nEFs on Si-substrates up to a resolution of ~5 microns. The high heat of reaction, low initiation temperature and excellent pressure-time characteristics of the nEFs, and their high-resolution micropatterning on Si-substrate has enabled them useful in pyrotechnics.

Keywords: Bismuth Oxide, Thin Films, Nanoenergetic Materials, Nanothermites, Micropatterning, Shadow masking

I. Introduction

Nanoenergetic materials comprising nanoscale homogeneous mixture of one of the oxidizer (CuO,[1-2] Bi_2O_3,[1] WO_3,[1] MoO_3[1] etc) with metal fuel (Al) are found to be of significant importance

in the development of pyrotechnics, propellants and explosives. Properties like ability to get deposited on flat substrates and also their patternability is of high significance for these materials as it enables some of these materials to develop Si-based safe initiator chip for timed detonation of safe arm and fire devices etc.[3] Nanoenergetic materials exothermally react to convert their chemical energy into mechanical and thermal energy thus producing high speed self-propagating combustion reactions and also shock waves if coupled to a suitable medium.[4] Packed or patterned nanoenergetic materials are suitably utilized in various applications such as safe arm fire devices,[3] microthrusters[5] molecular gene delivery[6] as well as pyrotechnic microinitiators[7] etc. Such applications can be easily realized by integrating patterned nanoenergetic materials with CMOS technology. Aluminum is basically used as a fuel particle in combination with several metal oxides such as CuO,[7-8] NiO,[9] and Co_3O_4[10] to realize nanoenergetic behavior. The oxidizer nanostructures of CuO/NiO/Co_3O_4 on MEMS devices have previously been fabricated by controlled oxidation of as-deposited Cu/Ni/Co thin films although most of this technology is confined to only dimension (thickness) being in the nanometer scale.[7-10] The power of standalone nanostructuring using molecular self assembly processes in terms of obtaining an overall nano-sized participation of the fuel and oxidizers has been explored by many groups. Bi_2O_3/Al based micro-chip initiator was reported recently,[11] in which the Bi_2O_3 nanoparticles were externally mixed with Al nanopowder and packaged on micro-chip which requires state of art packaging methodology. However, there were serious issues of bindability of such as-grown materials to the microchip surface for patterning aspects. Further if a ligand molecule is used to capture the patterns on the surfaces, it plays its own role in affecting the rate of burning and explosive performance of the nanoenergetic materials.

Bismuth oxide (Bi_2O_3) is a narrow band gap (2.8 eV) dielectric material having excellent electrical,[12] optical,[13] conducting[14] and catalytic[15] properties. A few developments in the synthesis of bismuth oxide nanostructures have been reported on glass substrate using chemical bath deposition[16] and Au-coated silicon substrate using atmospheric chemical vapor deposition[17] , thermal evaporation of bismuth oxide powder in a horizontal tube furnace under argon flow[18] etc. This inspired us to utilize this prior art knowledge to formulate nano-square-tablets of bismuth oxide using Noble metal (Au in our case) as catalytic agent followed by chemical bath deposition of Bi_2O_3. The catalytic behavior of such Nobel metals is well known and is principally due to enhanced interfacial charge transfer mechanism.[19] The nanoenergetic composite films of Bi_2O_3/Al were prepared by sputter deposition of aluminum on previously substrate grown Bi_2O_3 nanotablets using optimized deposition conditions. The exothermic reactivity of as prepared nanoenergetic films were examined by TG-DSC analysis from 50 to 800 ^{o}C in nitrogen atmosphere.

II. Experimental Section

A. Preprocessing of silicon substrates

A 500 μm thick silicon (p-type) wafer polished on both sides was sonicated for 30 min in acetone followed by rinsing using 2-propanol for 15 min. The wafer was further rinsed in deionized (DI) water and blow-dried with laboratory grade nitrogen gas followed by heating in a vacuum oven at 60 ^{o}C for 2 hr. A thin layer of insulating SiO_2 was grown on the cleaned silicon substrate at 1000 ^{o}C by wet oxidation technique using a batch top furnace (MRL Industries). The as-grown SiO_2 layer thickness (1 micron size) corresponding to a growth time of 4 hours was measured by Nanocalc (Ocean Optics).

B. LASER micromachining of PMMA mask

Polymethylmethacrylate (PMMA) mask was micromachined with a CO_2 pulse laser (M/S Epilog laser, USA). The designing of the intended micro pattern was carried out using Corel Draw. The drawing data was converted into a data exchange format which was used to drive the various stepper motors of the laser machine and all motions were confined to the x-y plane. The LASER machining was performed at room temperature under atmospheric pressure condition. The micromachining using laser was carried out on a 1 mm thick PMMA sheet at a scanning rate (vector mode) of 15 mm sec^{-1} laser speed, a laser power of 35 watt and laser frequency of 5 kHz. Further, wet chemical etching was performed on the laser cut samples with a mixture of acetone and ethanol at a ratio of 1:2 in ultrasonic bath set to 42 kHz frequency for 20 minutes. This helps us to achieve high cutting edge quality of the micromachined mask surface and edges.

C. PMMA masking of Si-substrate

A thin layer of sacrificial polydimethylsiloxane (PDMS) was spin coated on a glass slide for about 8-9 minutes at 8000 rpm using spin coater (M/S SPS-BV, Netherlands). The PDMS was prepared by mixing the prepolymers (M/s Dow Corning, Midland) in a ratio of 10:1 by weight with a curing agent. The bottom surface of the mask was stamped on to this coated PDMS for about 5 seconds and a thin layer (~1-2 μm) of PDMS is sheared from the parent film and adheres to the PMMA mask as the PMMA mask is separated from the parent film. This PDMS is tacky which furnishes this layer transfer process. This layer is used as an adhesive and sandwiches between the mask superimposed on the silicon substrate. This assembly is cured at 90 ^{o}C for about 15 min and this holds the mask tightly to the substrate. We have further performed a leak test on this assembly by pouring a red-dye and observing the optical patterns with optical microscope (Nikon 80i).

D. Synthesis of Bi_2O_3 NSTs and Realization of nEFs

The SiO_2 layered substrates with and without the PMMA mask were sputter coated with a 2 nm layer of titanium using a dual chamber sputtering-PECVD system NSP4000 (Nanomaster Inc.). The sputtered layer was obtained at 160 W power, 2.5 mTorr argon pressure and 20 sccm of argon flow rate. The sputtering was further followed by another layer of thickness 5 nm of gold as a stack (sputtering power of 200 W, argon flow rate of 20 sccm and pressure of 8 mTorr). Bismuth oxide nano-square-tablets were prepared by successive dipping of the Au-coated silicon substrate in two separate precursor solutions for 15 seconds followed by rinsing with water in between the dipping steps. The first precursor solution containing bismuth hydroxyl ions of pH 10 was prepared by adding 0.1 mol bismuth nitrate in a solution containing 5 ml concentrated (70%) nitric acid and 95 ml deionised water followed by drop by drop addition of NaOH. The second precursor solution containing hydrogen ions was made of 1 % hydrochloric acid. The first precursor solution was magnetically stirred throughout the deposition process and fresh deionised water was used after each cycle of deposition. The Bi_2O_3/Al nEFs were prepared by sputter deposition of aluminum onto the as-prepared Bi_2O_3 NSTs under argon pressure of 5 mTorr, argon flow rate of 20 sccm at sputtering power of 200 W. The sputtering layer (Ti/Au/Al) thickness was measured by the thickness monitor of sputtering-PECVD system, NSP4000.

E. Material characterization

The structural morphology of as prepared Bi_2O_3 NSTs and Bi_2O_3/Al nEFs on Au-sputtered Si substrate were characterized by field-emission scanning electron microscopy (Supra 40 VP, Zeiss Germany) and powder X-ray diffraction pattern using X´Pert Pro diffractometer

(PANanalytical, Netherlands) in 2θ range of 20-70° at scan rate of 0.02 s^{-1} with Cu Kα radiation of wavelength 1.5418 Å. The Bi_2O_3 NSTs on silicon substrate was characterized by FT-IR spectroscopy *via* Perkin-Elmer Spectrum from wave number 400 cm^{-1} to 4000 cm^{-1}. The thermo-gravimetric mass changes and heat of reaction of Al-sputtered Bi_2O_3 NSTs were characterized by thermo-gravimetry and differential scanning calorimetric (TG-DSC) studies carried on Netzsch STA 449F3 instrument. The TG-DSC analysis was conducted from 50 to 800 ^{o}C at a heating rate of 10 ^{o}C/min under nitrogen gas (99.999 % purity) environment flowing at 20 ml/min.

The pressure and pressurization rate of nanoenergetic composites was measured by conducting the combustion experiment of 15 mg of Bi_2O_3/nAl composites in a constant volume pressure-cell (diameter=6.25 mm, depth=2.5 mm) as shown in Fig. 1. A piezoelectric pressure sensor PCB 119B12 (PCB Piezotronics) was rigidly fixed to the pressure-cell to measure the pressure-time characteristics of the combustion which was recorded by Tektronix digital oscilloscope (DPO3054).

III. Results and Discussions

The X-ray diffraction patterns of as-grown Bi_2O_3 NSTs on gold coated Si substrate with a stacked aluminum are shown in Fig. 2. The consistency of all the XRD peaks with JCPDS standard (41-1449) of bismuth oxide with a monoclinic phase is clearly reflected in Fig. 1. The peaks of titanium and gold are visible in the XRD and no peak related to hydroxide is detected. The XRD peaks and EDX measurements of nanoenergetic films is represented by Fig. 3. Fig. 3 clearly denotes the presence of peaks corresponding to the elements Ti, Au and Al which endorses the data reflected by XRD measurements in Fig. 2. The morphology and structure of as-synthesised bismuth oxide on bare as well as Au-sputtered Si substrate was studied by

FESEM. It was observed that micro-leaf like structure of bismuth oxide could be formulated on bare silicon substrates as shown in Fig.4 (a). Substrates with Ti/Au stacks reflected the formulation of bismuth oxide nano-square-tablets which does not come in the absence of Au/Ti stack. This strongly endorses the basis of such formulations. Fig. 4 (b) and (c) show the formation of nano-square-tablets of bismuth oxide on Au-sputtered Si-substrate having average edge length of 200-300 nm and thickness of 50-100 nm. Fig. 4 (d) represents the FESEM image of nanoenergetic films of Bi_2O_3 NSTs with sputtered-aluminum of thickness around 100 nm.

The Fourier transform infrared spectrum (FT-IR) of thin film of Bi_2O_3 NSTs on silicon substrate is obtained and shown in Fig. 5.The band at wave number 1074.9 cm^{-1} is attributed to the stretching vibrations of Si-O bond[20] indicating the presence of SiO_2 layer at the interface between deposited thin film of Bi_2O_3 NSTs and the silicon substrate. The low vibration modes observed at wave number of 465.11 cm^{-1} and 610.69 cm^{-1} can be related to the representative peak of the vibration of the bond Bi-O of distorted BiO_6 octahedral structural unit.[21-22] The frequency band at wave number 818.83 cm^{-1} can be assigned to the stretching vibration of Bi-O bond of BiO_3 species from BiO_6 octahedron.[23]

The mechanism of formation of bismuth oxide structure on silicon chip in terms of the reaction mechanism has been described earlier by Pathan *et al*.[24] In our case we hypothesize an identical behavior. When the silicon chip is immersed into the first precursor solution, the bismuth hydroxyl ions gets adhered to the chip due to possible van der Waals attraction forces or electrostatic forces between hydroxylation surface of SiO_2 owing to the presence of water in the precursor and the bismuth hydroxyl groups. The adsorbed bismuth hydroxyl ions on chip

when immersed in the second solution, react with hydrogen ions and form bismuth oxide structure as per Equation-1 below.

$$2\ Bi(OH)_4^- + 2\ H^+ \longrightarrow Bi_2O_3 + 5\ H_2O \text{---------(1)}$$

The water rinsing of chip removes the loosely bound or unreacted molecules. The crystal growth of bismuth oxide proceeds layer by layer and the growth kinetics depend on the precursor concentration, deposition time and number of cycles. The gold nanoparticles on the surface of Au-sputtered silicon wafer acts as a catalyst by performing as a sink for interfacial charge transfer as they come in contact with the hydroxyl ions. Therefore, these then act as metalized centers to promote grain growth and nucleation for the favorable growth of bismuth oxide nanocrystals. It has been observed that owing to the minuscule total thickness of the stack the gold gets deposited as a discontinuous layer which gives us a basis of hypothesizing for nucleating gold sites as detailed above. This interfacial interaction of gold and bismuth oxide nanostructure enhances the colloidal bond stability as well as room temperature stability for favorable nanocrystals growth from this catalyst sites.

The TG-DSC studies of heat released during the thermite reactions of 60, 100 and 140 nm aluminum sputtered nEFs has been shown in Fig. 6 a, b and c. Among all three TG-DSC measurement studies, 140 nm Al-sputtered nEFs has developed highest heat of reaction (ΔH_r) of 710 J/g (peak temperature (T_p) of 589 ^oC) as well as also initiated at a lowest onset temperature (T_{on}) of 535 ^oC compared to 60 nm-Al sputtered (T_{on}=540 ^oC, ΔH_r = 180 J/g) and 100 nm-Al sputtered (T_{on}=550 ^oC, ΔH_r = 209 J/g) nEFs. The residual mass of nEFs formulated with aluminum sputter-layer of 60, 100 and 140 nm was 108.4%, 103.2 % and 100.2 % respectively in thermo-gravimetric studies of these samples. From thermo-gravimetric and DSC observations, it may be interpreted that the aluminum sputter-layer of 140 nm has furnished

nearly optimum requirements of fuel for about complete combustion of Bi_2O_3 oxidizers. The endothermic peaks in all three nEFs with aluminum sputter-layer of 60, 100 and 140 nm have been observed at onset temperature of 645, 642 and 646 ^oC respectively with a corresponding endothermic heat magnitude of 17, 19 and 18 J/g. The almost similar trends in initiation and heat magnitude of endothermic peaks of all three nEFs can be attributed to the melting of aluminum. The thermo-gravimetric mass is observed decreasing up to about 460 ^oC, which may be attributed to occur due to possible consequence of thermal decomposition of bismuth trioxide and evaporation of any moisture adsorbed by bismuth trioxide. In thermo-gravimetric analysis of all three nEFs, the thermo-gravimetric mass was observed to start increasing from about 460 ^oC exhibiting a residual mass above 100 %, which can be attributed to the reaction of aluminum[25] with small residual oxygen contained as impurity (<0.001%) in nitrogen gas and the reaction of titanium[26] with nitrogen in the temperature range of ~ 460-650 ^oC. A similar trend of increasing of thermo-gravimetric mass from around 600 ^oC was observed during TG analysis of Al/Co_3O_4 nanoenergetic materials due to reaction of aluminum with small content oxygen present in the argon gas.

Owing to highest magnitude of heat of reaction of DSC measurement of nEFs obtained due to nearly best combination of Bi_2O_3 NSTs with 140 nm sputter-layer of aluminum, this nEFs has been selected for pressure-time characteristics measurement. The combustion was performed by blasting the scratched nEFs in a pressure cell experiment at a charge density of 0.2 g cm^{-3}. The pressure-time characteristics measurement has been shown in Fig. 7. In pressure-time characteristics measurement, the peak pressure and its pressurization rate was measured to be 40.8 MPa and 4.08 MPa μs^{-1}. This pressurization rate is remarkably higher than that achieved by the combustion of the same charge density of nanothermite composites of aloe-assisted CuO

nanorods and aluminum.[2] The higher gas generating ability of this nEFs has contributed in enhancing rate of rise of peak pressure and hence the pressurization rate. The higher gas generating ability and so the higher pressure built up capability has been observed in other research findings also.[27-28]

A micropatterning trial of this process is carried out by realizing a mask of PMMA with lines of width of 200 microns obtained through laser micromachining of PMMA substrate of 1 mm thickness. The micromachined PMMA sheet with PDMS layer transferred by stamping and sticking bonding technique[29] is used as a shadow mask throughout the deposition process including the deposition of the Ti/Au stack, the aqueous chemical formulation of the NSTs of Bismuth oxide and also the aluminum coating of the Bi_2O_3 NSTs. Fig. 8 (a) shows the titanium and gold sputtered photo images of PMMA masked silicon substrates with the bottom layer of silicon substrate and top layer of PMMA mask. The PMMA masked silicon substrate shows no leakage during the florescent die leak test (Fig. 8 b) which clearly interprets that the PMMA mask was perfectly aligned and sealed with silicon substrate. Fig. 8 (c) and (d) shows the FESEM micrographs of the patterned nanoenergetic composites comprising of Bi_2O_3 NSTs and a sputter coated aluminum layer. Fig. 8 (e) and (f) reflects the FESEM image of 60° inclined nEFs of Bi_2O_3/Al (Aluminum sputter layer of 60 nm) micropatterned on silicon substrate. From Fig. 8 (c) and (e), it can be interpreted that the Bi_2O_3/Al nanoenergetic films have been formulated with variable deposition thickness of Bi_2O_3 however, from high magnification FESEM image Fig 8 (f) (Magnified FESEM view of encircled section of Fig. 8e), the Bi_2O_3/Al is measured of 320±30 nm. From the FESEM observation, the Bi_2O_3 layer can be approximated to be of 260±30 nm. The width of an individual composite pattern is found as 203±4 μm whereas the width of the mask holes is 205±2 μm. This shows a repeatability of patterning

within ±4 μm accuracy which illustrates good resolution and localization according to the shadow guidance given by the mask. This indicates the relevancy of this process towards micro-patterning of these composites which can be utilized for micro-chip initiators, detonators, microthrusters and other pyrotechnic applications related to micro-chip manufacture.

IV. Conclusions

Uniform and symmetric nanosquaretablets of Bi_2O_3 have been synthesized on silicon substrate by catalytic assistance of gold nanoparticles. The gold nanoparticles are supposed to act as a favorable active crystal sites for the stable colloidal growth of bismuth trioxide NSTs. In the absence of gold film on silicon substrate, instead of Bi_2O_3 NSTs, micro-leaf structures are formed. The FT-IR spectroscopy of the deposited thin film of Bi_2O_3 NSTs on silicon substrates have shown the representative peaks of SiO_2 interfacial layer between the Bi_2O_3 NSTs and Si substrate as well as the vibration bands of Bi-O bond. Bi_2O_3/Al based nanoenergetic films have been realized by sputtering of aluminum of varied sputter-layer thickness of 60, 100 and 140 nm over chemically grown Bi_2O_3 NSTs. TG-DSC characterizations of Bi_2O_3/Al based nEFs shows that the exothermic reaction initiates before the melting of aluminum based on solid-phase diffusion mechanism. The nEFs formulated by 140 nm sputter deposition of aluminum has shown to develop highest magnitude of heat of reaction (710 J/g), initiated at an onset temperature (535 ^{o}C) in TG-DSC measurement. This nanoenergetic films is able to generate a very high pressurization rate of 4.08 MPa μs^{-1} and a moderate peak pressure of 40.8 MPa in combustion experiment in constant volume pressure-cell at a charge density of 0.2 g cm^{-3}. Further micro-patterning of these composites is carried out and it is observed that good patterning resolution can be obtained through this deposition process. This makes the process a

promising candidate for manufacture of functional micro/nano devices in silicon for a variety of pyrotechnic applications.

Acknowledgements

We sincerely thanks to Science Engineering and Research Council, Department of Science and Technology (DST), Government of India for its financial support. The author would also like to acknowledge Nanoscience and Soft Nanotechnology Centre, IIT Kanpur for providing good material characterization facilities. The authors also thank Netzsch Technologies India Pvt Ltd Chennai for its TG-DSC measurements.

References

1 V. E. Sanders, B. W. Asay, T. J. Foley, B. C. Tappan, A. N. Pacheco, and S. F. Son, *J. Propul. Power*, 2007, **23**, 707-714.

2 V. K. Patel, and S. Bhattacharya, *ACS Appl. Mater. Interfaces*, 2013, **5**, 13364-13374.

3 C. Rossi, S. Orieux, B. Larangot, T. D. Conto, and D. Esteve, *Sens. Actuators, A,* 2002, **99**, 125-133.

4 S. Apperson, R. V. Shende, S. Subramanian, D. Tappmeyer, S. Gangopadhyay, Z. Chen, K. Gangopadhyay, P. Redner, S. Nicholich, and D. Kapoor, *Appl. Phys. Lett.,* 2007*,* **93***,* 243109.

5 H. Pezous, C. Rossi, M. Sanchez, F. Mathieu, X. Dollat, S. Charlot, L. Salvagnac, and V. Conedera, *Sens. Actuators, A,* 2010*,* **159**, 157-162.

6 M. Korampally, S. J. Apperson, C. S. Staley, J. A. Castorena, R. Thiruvengadathan, K. Gangopadhyay, R. R. Mohan, A. Ghosh, L. Polo-Parada, and S. Gangopadhyay, *Sens. Actuators, B,* 2012, **171-172**, 1292-1296.

7 K. Zhang, C. Rossi, G.A.A. Rodriguez, C. Tenailleau, and P. Alphonse, *Appl. Phys. Lett.,* 2007, **91,** 113117**.**

8 M. Petrantoni, C. Rossi, V. Conedera, D. Bourrier, P. Alphonse, and C. Tenailleau, *J. Phys. Chem. Solids,* 2010*,* **71**, 80-83**.**

9 K. Zhang, C. Rossi, P. Alphonse, C. Tenailleau, S. Cayez, and J.-Y. Chane-Ching, *Appl. Phys. A,* 2009, **94**, 957-962.

10 Z. Qiao, D. Xu, F. Nie, G.Yang, and K. Zhang, *J. Appl. Phys.,* 2012*,* **112**, 014310.

11 C. S. Staley, C. J. Morris, R. Thiruvengadathan, S. J. Apperson, K. Gangopadhyay, and S. Gangopadhyay, *J. Micromech. Microeng.,* 2011, **21**, 115015 .

12 D.H. Bao, T.W. Chiu, N. Wakiya, K. Shinozaki, and N. Mizutani, *J. Appl. Phys.,* 2003, **93**, 497-503.

13 L. Leontie, J. *Optoelec. Adv. Mater.,* 2006, **8**, 1221-1224**.**

14 P. Shuk, H. D. Wiemhofer, U. Guth, W. Gopel,and M. Greenblatt, *Solid State Ionics,* 1996, **89**, 179-196.

15 N. Pugazhenthiran, P. Sathishkumar, S. Murugesan, and S. Anandan, *Chem. Eng. J.,* 2011*,* **168**, 1227-1233.

16 T.P. Gujar, V.R. Shinde, C.D. Lokhande, and S-*H. Han, Mater. Sci. Eng., B***,** 2006, **133**, 177-180.

17 X.-P. Shen, S.-K. Wu, H. Zhao, and Q. Liu, *Physica E,* 2007*,* **39**, 133-136.

18 M. Zhao, X.L. Chen, Y.J. Ma, J.K. Jian, L. Dai, and Y.P. Xu, *Appl. Phys. A*, 2004, **78**, 291-293.

19 P.V. Kamat, and D. Meisel, *Curr. Opin. Colloid Interface Sci.*, 2002, **7**, 282-287.

20 P.G. Pai, S.S. Chao, Y. Takagi, and G. Lucovsky, *J. Vac. Sci. Technol.,*1986*,* ***A*4**, 689-694 .

21 P. S. Rao, C. Rajyasree, A.R. Babu, P.M.V. Teja, and D. K. Rao, *J. Non-Cryst. Solids,* 2011*,* **357**, 3585-3591.

22 M. Bosca, L. Pop, G. Borodi, P. Pascuta , and E. Culea, *J. Alloys Compd.,* 2009*,* **479**, 579-582 **.**

23 F. He, J. Wang, and D. Deng, *J. Alloys Compd.,* 2011**, 509**, 6332-6336.

24 H. M. Pathan, and C.D. Lokhande, *Bull. Mater. Sci.,* 2004**, 27**, 85-111.

25 D. Xu, Y. Yang, H. Cheng, Y. Y. Li and K. Zhang, *Comb. Flame*, 2012, **159**, 2202-2209.

26 J. Nulmain, *U. S. Patent*, 5236868, 1993.

27 J. A. Puszynski, C. J. Bulian and J. J. Swiatkiewicz, *J. Propul.Power,* 2007, **23**, 698-706.

28 K. S. Martirosyan, *J. Mater. Chem.,* 2011, **21**, 9400-9405.

29 S. Satyanarayana, R. N. Karnik, and A. Majumdar, *J. Microelectromech. Syst*., 2005, **14**, 392-399.

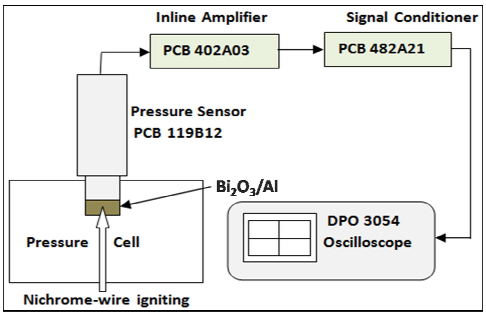

Fig. 1 Pressure-Time Characteristics Measurement Setup

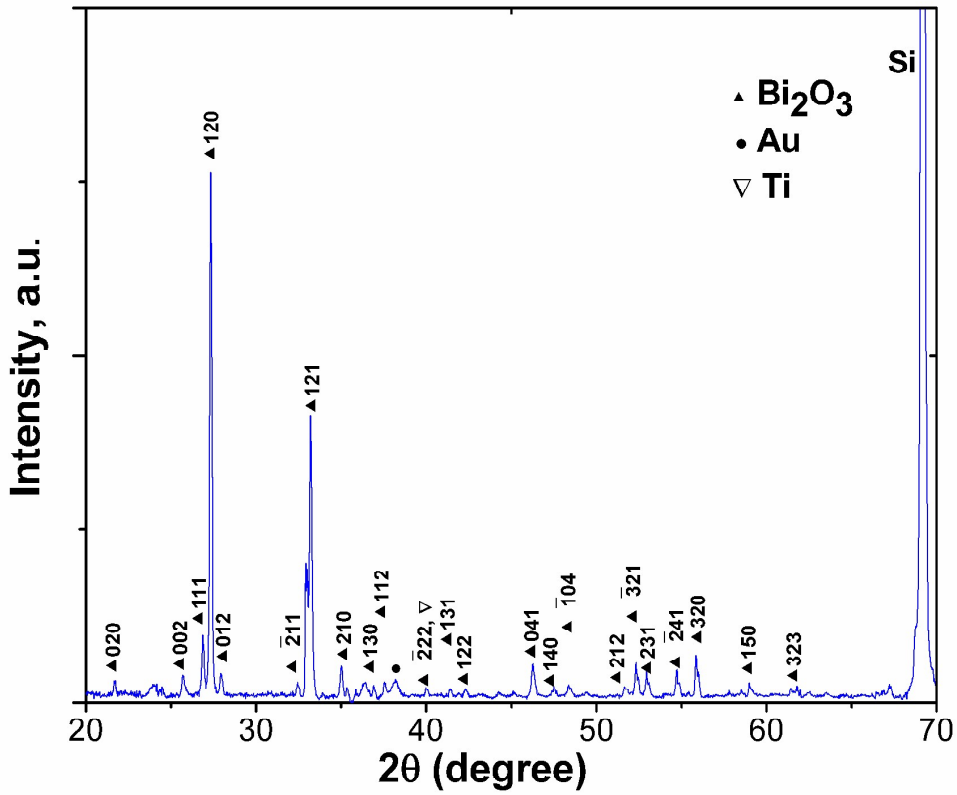

Fig.2 X-ray diffraction pattern of Bi_2O_3 NSTs on silicon substrate

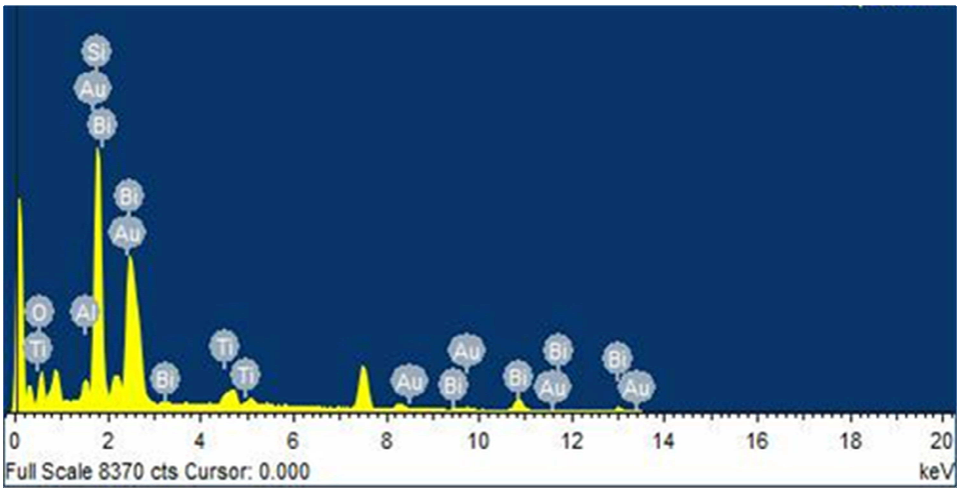

Fig. 3 EDX measurements of Bi_2O_3 NSTs/Al nEFs.

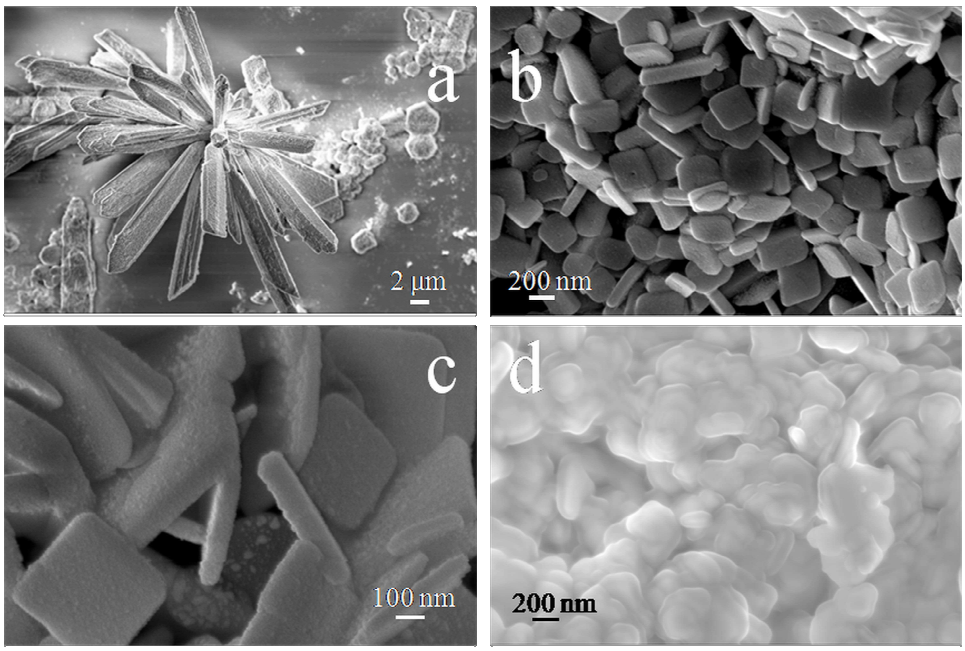

Fig.4. FESEM image of (a) Bi_2O_3 micro-leaf structures (b, c) Bi_2O_3 NSTs (d) Bi_2O_3 NSTs/nano-Al nEFs, on Au-coated Si substrate

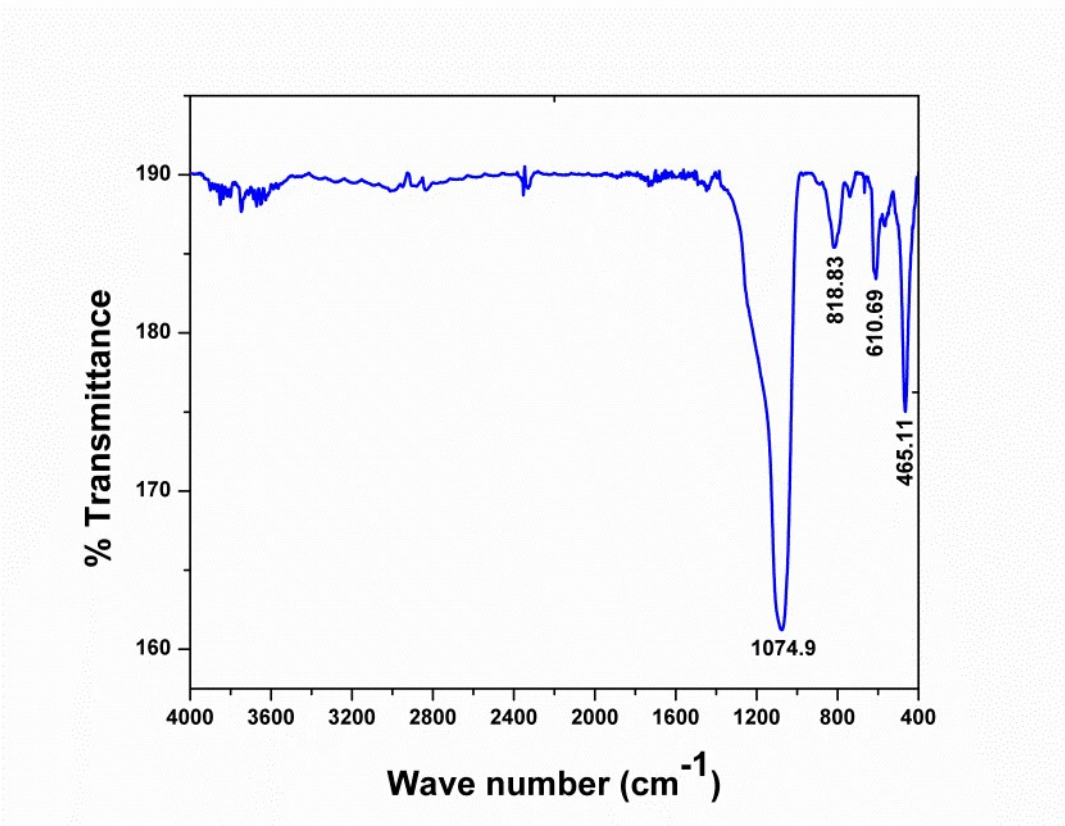

Fig. 5. FT-IR spectrum of Bi_2O_3 NSTs on silicon substrate

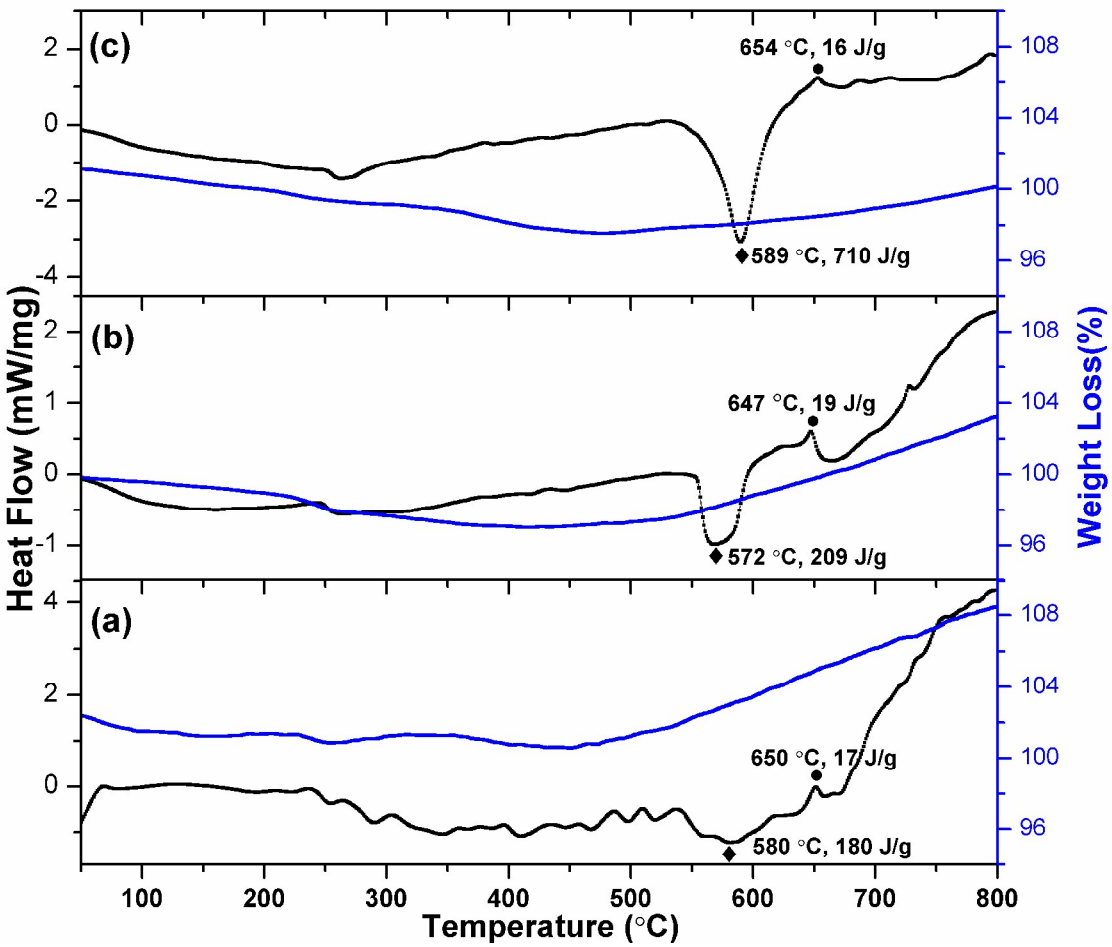

Fig. 6. TG-DSC measurements of nanoenergetic films of Bi_2O_3 NSTs/Al with varied aluminum sputter-layer of (a) 60 nm, (b) 100 nm and (c) 140 nm

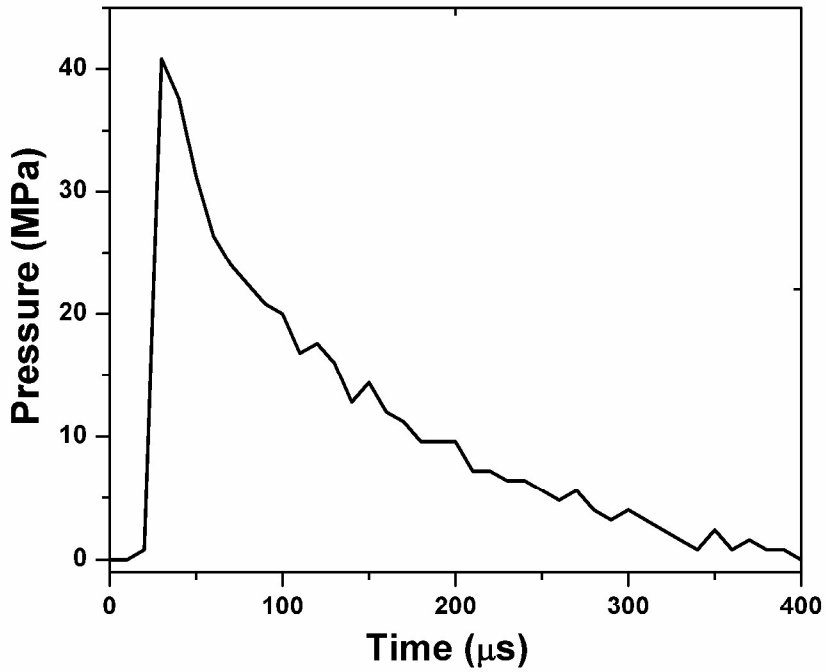

Fig.7 Pressure-time characteristics measurement of Bi_2O_3/Al nEFs having Al-sputter layer of 140 nm

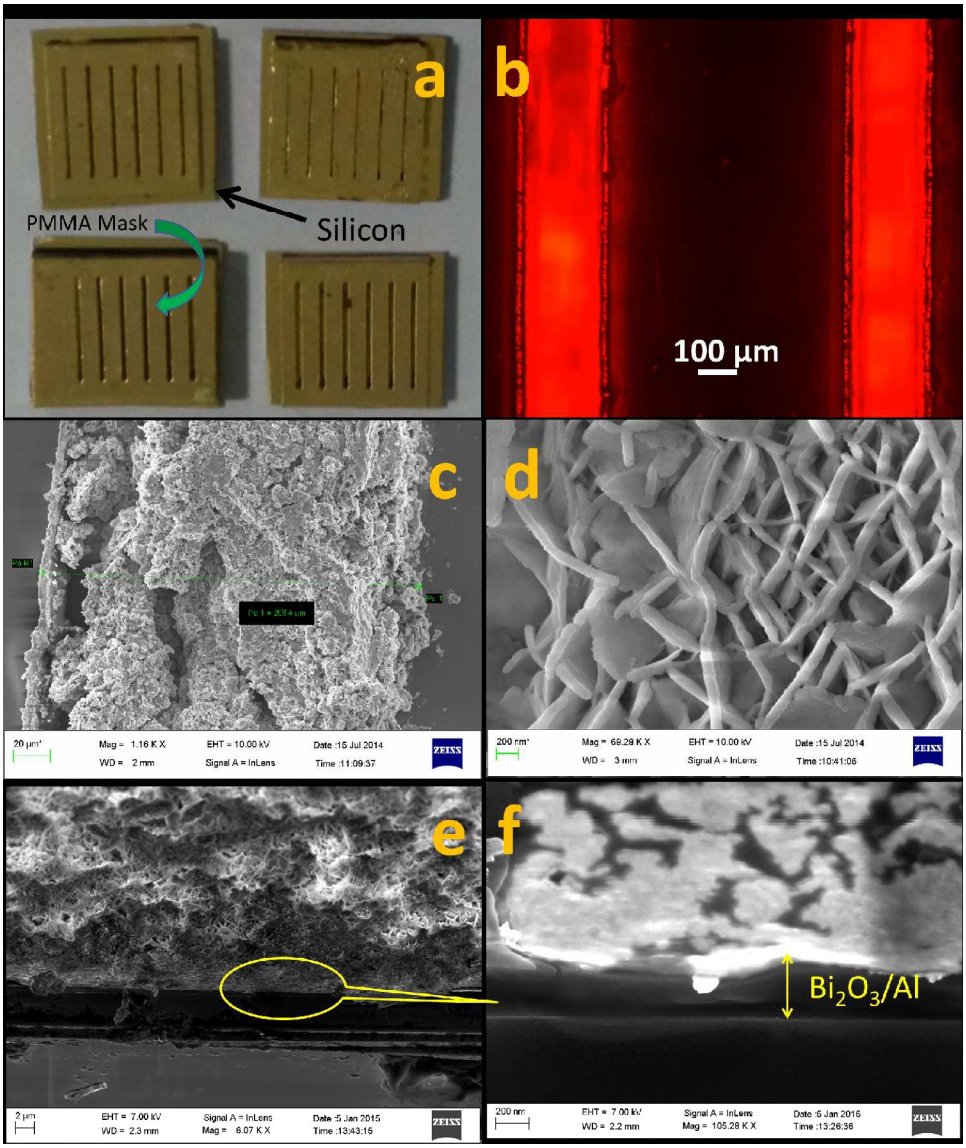

Fig. 8 (a) Image of Ti and Au-sputtered PMMA masked Si-substrates (b) Fluorescent dye leak test image of mask-channels (c, d) FESEM image of micropatterned Bi_2O_3/Al nEFs (e) FESEM image of inclined micropatterned Bi_2O_3/Al nEFs (f) High magnification FESEM image of encircled section of image 8 (e) showing Bi2O3/Al deposition layer of 310 nm for aluminum sputter layer deposition of 60 nm

Table of Contents

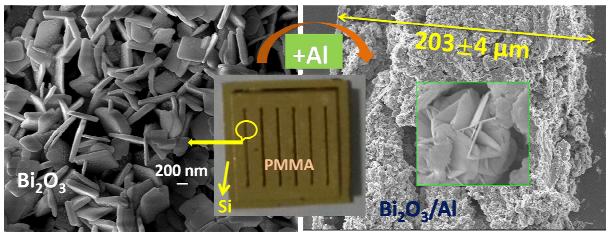

Nanoenergetic films of Bi_2O_3/Al are micropatterrned at a high resolution of ~5 microns on silicon substrate exhibiting high heat of reaction, low initiation temperature and excellent pressure-time characteristics for pyrotechnics applications.